European Symposium on Computer Aided Process Engineering – 15
L. Puigjaner and A. Espuña (Editors)

Nonlinear Approach to Design of Monolithic Loop Reactor for Fischer-Tropsch Synthesis

Montree Lumluksanaphaiboon, Costin Sorin Bildea* and Johan Grievink
Delft University of Technology,
Julianalaan 136, 2628BL Delft, The Netherlands

Abstract

The nonlinear behaviour of the monolithic loop reactor for Fischer-Tropsch synthesis is investigated. The model consists of non-stationary mass balance in gas, liquid and solid (catalyst) phases, together with energy balance. If the external heat-exchanger is small, the system exhibits multiple steady states and the moderate-conversion state is unstable. Due to occurrence of Hopf bifurcations, only parts of the high- and low-conversion states are stable. State multiplicity disappears for a large heat exchanger. However, sustained oscillations occur around desired operating points. By calculating relevant bifurcation varieties, the reactor can be designed such that the reaction ignition / extinction and the oscillatory behaviour are avoided, even when the design parameters are uncertain or the plant is subjected to disturbances. A control structure is proposed, as an alternative solution for achieving stable operation.

Keywords: Fischer-Tropsch, monolithic reactor, design, multiplicity, Hopf bifurcations

1. Introduction

As the reserves of crude oil are depleted and its price rises, conversion of synthesis gas to fuels and chemicals becomes of increasing interest. In Fischer-Tropsch synthesis, a mixture of hydrocarbons, from methane to heavy waxes, is obtained. The highly exothermal reaction is performed using cobalt or iron-based catalysts. The temperature and H_2 / CO ratio must be kept within narrow ranges, because of selectivity requirements. Typical reactors include fluidized bed, slurry bubble columns and multi-tubular fixed bed reactors. Recently, de Deugd et al (2003) proposed the monolithic loop reactor (Figure 1) as an alternative. Steady state results showed that such a reactor, operated at 10-30 bar and 200 - 240 ºC, has a competitive size and achieves high productivity and selectivity.

This work addresses the dynamics and control of a Fischer-Tropsch process which employs the monolithic loop reactor. The investigation is justified by the experimental observation (Song et al, 2003a) of reaction ignition in a stirred tank slurry reactor, manifesting as a switch to the methane-forming mode. This undesired incident was explained by the decrease of heat removal performance, in a system which has multiple steady states. The analysis was extended (Song et al, 2003b) to bubble columns.

* Author to whom correspondence should be addressed: c.s.bildea@tnw.tudelft.nl

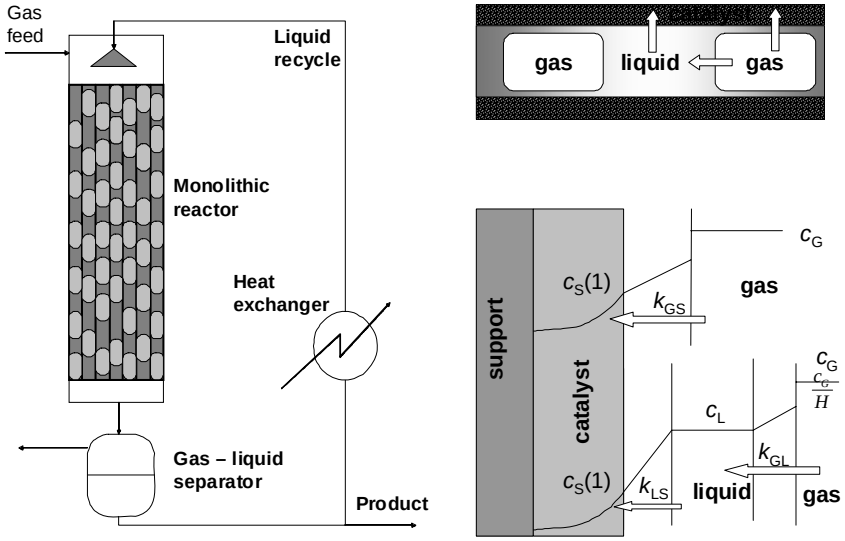

Figure 1. The monolithic loop reactor for Fischer-Tropsch synthesis

In the present work, we show that the monolithic loop reactor performing the Fischer-Tropsch synthesis also exhibits state multiplicity, when the external heat-exchanger is small. This has to be avoided, because the interesting middle-conversion state is unstable. State multiplicity disappears for larger heat exchangers, but sustained oscillations occur around the desired operating points. Very large heat transfer areas are necessary to guarantee state unicity and stability. Alternatively, a control structure is proposed, to stabilize the unstable operating points.

2. Model assumptions and equations

The monolithic loop reactor is presented in Figure 1. The catalyst consists of long parallel channels, separated by thin walls. A simplified scheme of the mass transfer between the three phases in the catalyst channel is also shown in Figure 1. The reactor is fed with fresh synthesis gas mixed with liquid products, in order to a) limit the temperature rise; and b) achieve Taylor flow pattern consisting of alternating gas bubbles and liquid slugs. H_2, CO and light products are mainly in the gas phase, while heavy products are in the liquid phase. Gas-liquid, gas-solid and liquid-solid mass transfer is enhanced due to the thin liquid film between bubbles and catalyst and the recirculating flow within the liquid slugs. At reactor outlet, the liquid product is separated, and partially recycled to reactor inlet after cooling.

Due to space limitations, the dimensionless model will be discussed briefly. c, θ, ξ and τ are dimensionless concentrations, temperature, axial coordinate and time, respectively. CO and H_2 balance in the gas and liquid phases Eqs (1) and (2) assume plug flow. u_G and u_L are the superficial velocities of the gas and liquid phases, respectively. The equilibrium at the gas-liquid interface is modelled with Henry's law, with temperature-dependent coefficients H_i estimated from the experimental data of Wang et al (1999).

Mass transfer coefficients from gas to liquid (ω_{GL}), gas to solid (ω_{GS}), and liquid to solid (ω_{LS}) are calculated following Kreutzer et al (2001). The hydrocarbons formed in the reactions are lumped into "lights" and "heavies", which are found only in the gas and liquid phase, respectively. To calculate the stoichiometric coefficient of the light hydrocarbons used in equation (3), we assumed product selectivity following the AFS distribution, and performed vapour-liquid equilibrium calculations in AspenPlus using Peng Robinson model. The superficial liquid velocity u_L is assumed to be constant, because the amount of hydrocarbons formed by reaction is small compared to the liquid recycle. The change of the gas superficial $\partial u_G/\partial\tau$ is calculated from the overall mole balance over the gas phase (summation of Eqs 1 and 3, not shown here). The rates of change of the gas superficial velocity u_G and of the void fraction ε are related by equation (4). The Damkohler number *Da* contains the reaction rate constant at reference conditions, feed flow rate and reactor volume. Solution of diffusion – reaction equations within the catalyst layer of thickness λ showed that the resistance to mass transfer can be neglected. Therefore, the balance within the catalyst is represented by the steady-state Eq. (5). The energy balance Eq. (6) assumes constant heat of reaction β, accounts for the solid heat capacity through the Lewis number *Le*, and neglects the heat capacity of the gas. The kinetic equation (7) is based on experimental data of Yates and Satterfield (1991), with parameters estimated by Maretto and Krishna (1999). The reactor-inlet and reactor-outlet temperatures, $\theta(0)$ and $\theta(1)$ respectively, are coupled through Eq. (8), where ε_{HE} and θ_c are heat exchanger efficiency and coolant temperature, respectively.

$$\frac{\partial \varepsilon c_{i,G}}{\partial \tau} = -\frac{\partial u_G c_{i,G}}{\partial \xi} - \omega_{GL,i}\left(\frac{1}{H_i}c_{i,G}(1+\theta) - c_{i,L}\right) - \varepsilon\omega_{GS,i}\left(\frac{1}{H_i}c_{i,G}(1+\theta) - c_{i,S}\right) \quad (1)$$

$$\frac{\partial (1-\varepsilon) c_{i,L}}{\partial \tau} = -\frac{\partial u_L c_{i,L}}{\partial \xi} + \omega_{GL,i}\left(\frac{1}{H_i}c_{i,G}(1+\theta) - c_{i,L}\right) - \omega_{LS,i}(1-\varepsilon)\left(c_{i,L} - c_{i,S}\right) \quad (2)$$

i = CO, H2

$$\frac{\partial \varepsilon c_{j,G}}{\partial \tau} = -\frac{\partial u_G c_{j,G}}{\partial \xi} + \nu_j \cdot \lambda \cdot Da \cdot r \quad (3)$$

j = lights, H_2O

$$\frac{\partial \varepsilon}{\partial \tau} = \frac{u_L}{(u_G + u_L)^2} \cdot \frac{\partial u_G}{\partial \tau} \quad (4)$$

$$Da \cdot \lambda \cdot \upsilon_i \cdot r = \omega_{GS,i} \cdot \varepsilon \cdot \left(\frac{1}{H_i}c_{i,G}(1+\theta) - c_{i,S}\right) + \omega_{LS,i} \cdot (1-\varepsilon) \cdot \left(c_{i.L} - c_{i,S}\right) \quad (5)$$

$$\frac{\partial (Le - \varepsilon)\theta}{\partial \tau} = -\frac{\partial u_L \theta}{\partial \xi} + \lambda \cdot Da \cdot \beta \cdot \nu_{CO} \cdot r \quad (6)$$

$$r = \frac{\exp\left(\frac{\gamma_a \theta}{1+\theta}\right) \cdot c_{CO,S} \cdot c_{H_2,S} \cdot (1+\theta)^2}{\left(1 + B \cdot \exp\left(-\frac{\gamma_b \theta}{1+\theta}\right) \cdot c_{CO,S} \cdot (1+\theta)\right)^2} \tag{7}$$

$$\theta(0) = (1-\varepsilon_{HE}) \cdot \theta(1) + \varepsilon_{HE} \cdot \theta_c \tag{8}$$

3. Steady state and dynamic behaviour

The steady state model is obtained by dropping the time derivatives in Eqs (1) - (8). The boundary-value problem is solved by shooting. The dependence of the steady state solution versus one parameter is obtained by a continuation algorithm based on local parametrization. Figure 2 presents typical conversion versus coolant temperature bifurcation diagrams. Generally, the system shows multiple steady states when the efficiency of the external heat exchanger is low. The multiplicity and unicity regions are separated by fold bifurcation points, which are represented by the bold line in Figure 2. Note that the middle-conversion state is unstable, because the well-known slope stability condition is not fulfilled.

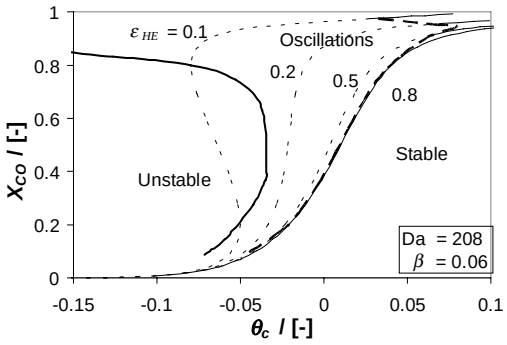

Figure 2. CO conversion versus coolant temperature bifurcation diagrams.

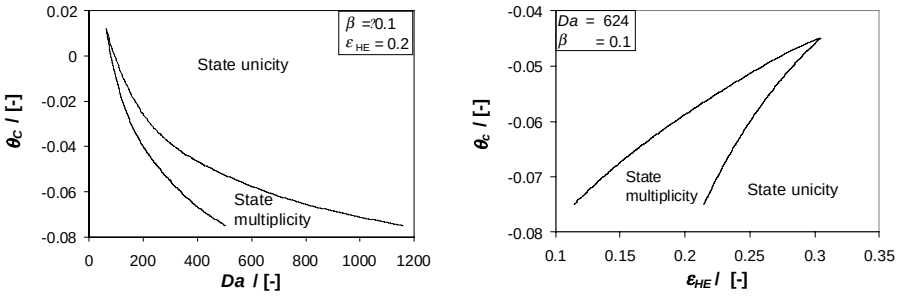

Figure 3. Locus of singular points, bounding the multiplicity region

Figure 3 shows in $Da - q_c$ and ε_{HE} - q_c diagrams the locus of the singular points, which bound the region where multiple states exist. In general, small reactors, large coolant temperature and high heat transfer area are favourable for state unicity.

The full dynamic model is necessary to analyze the stability of the high- and low-conversion steady states. The model is solved by the method of lines. It turns out that the high- and low-conversion operating points may be unstable. Figure 4 presents results of dynamic simulations, with initial conditions close to the low- intermediate- and high-conversion states, (denoted by L, M, and H, respectively). The onset of a large limit cycle is evident. Such oscillations also occur for parameter values in the unicity region. The oscillations, explained by the wrong-way behaviour of the reactor coupled with the positive feedback due to energy recycle, should be avoided in practice. Note that the stability of the stationary point is lost and a limit cycle is simultaneously born at Hopf bifurcation points, represented by the dashed bold line in Figure 2. The high value of the heat exchanger efficiency, ε = 0.8, which guarantees the stability of the whole solution branch, should also be remarked.

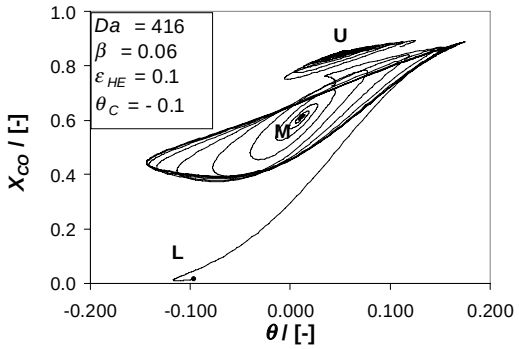

Figure 4. Dynamic simulation results showing limit cycle..

4. Control structure

Figure 5 shows a control structure that can achieve stable operation. The synthesis gas is on flow control. Because state multiplicity and instability are the result of positive feedback due to recycle, the control structure decouples the reactor inlet and outlet by a flow controller and a standard temperature control scheme for the heat exchanger (steam generator). Solution of the dynamic model (1) – (8) to which controller equations were added proved that stabilization of unstable operating points is possible, both in the multiplicity and in the unicity regions.

The control system must prevent runaway in the case of cooling failure. Although the highest temperature is normally at the reactor outlet, local hot spots could arise due to wrong-way behaviour during transients, or due to gas/liquid maldistribution. For these situations, an override structure is implemented. When the un-reacted syngas is recycled, a water-removal unit is installed and the amount of hydrocarbons at reactor-inlet is controlled via the purge flow rate.

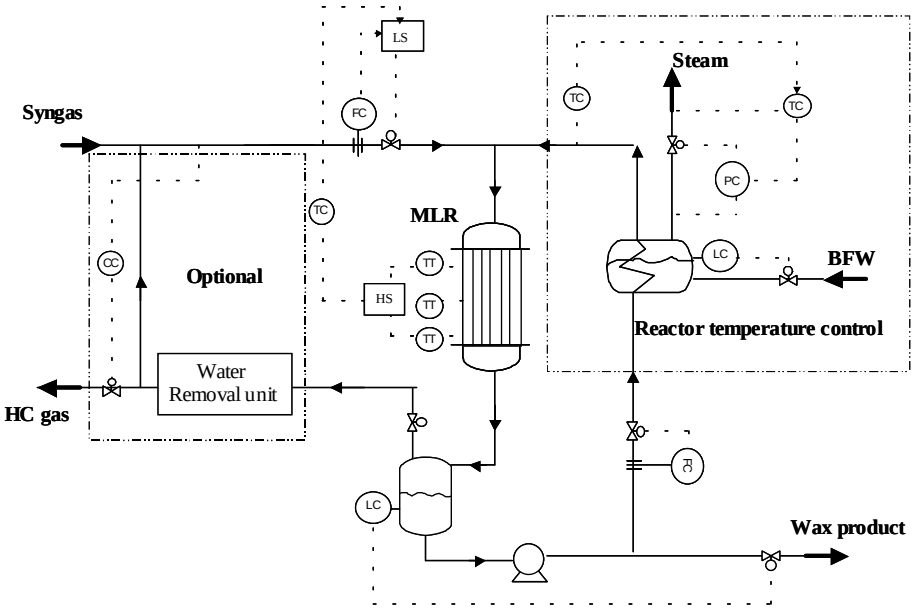

Figure 5. Control structure for Fischer-Tropsch synthesis in monolithic loop reactor

Conclusions

1. The monolithic loop reactor for Fischer-Tropsch synthesis may exhibit state multiplicity and instability (Figure 2).
2. Multiplicity can be avoided and stability can be ensured by changing the design parameters Da, β, ε_{HE} and θ_C.
3. Stable operation can also be achieved by control (Figure 5). Additionally, the control system should guard against reaction runaway in case of cooling failure.

References

de Deugd, R., Chougule, R., Kreutzer, M., Meeuse, M., Grievink, J., Kapteijn, F. and Moulijn, J., *Chem. Eng. Sci*, **58**, 583, 2001.
Kreutzer, M., Du, P., Heiszwolf, J., Kapteijn, F., Moulijn, J., *Chem. Eng. Sci*, **56**, 6015, 2001.
Maretto, C. and Krishna, R., *Catalyst Today*, **52**, 279, 1999.
Song, H., Ramkrishna, D., Trinh,S. and Wright, H., *AIChE .Journal*, **49**, 1803, 2003a.
Song, H., Ramkrishna, D., Trinh, S., Espinoza, R. and Wright, H., *Chem. Eng. Sci.*, **58**, 2759, 2003b.
Wang, Y.-N., Li, Y.-W., Bai, L., Zhao, Y.-L. and Zhang, B.-J., *Fuel*, **78**, 911, 1999.
Yates, Y.C. and Satterfield, C.N., *Energy & Fuels*, **5**, 168, 1991.